

Cubic phase gate operation to decrease the error of two-mode transformations

© E.R. Zinatullin¹, S.B. Korolev^{1,2}, T.Yu. Golubeva¹

¹ St. Petersburg State University, St. Petersburg, Russia

² South Ural State University (National Research University), Chelyabinsk, Russia

e-mail: e.r.zinatullin@mail.ru

Received November 08, 2023

Revised November 08, 2023

Accepted November 12, 2023

The paper considers a strategy to decrease the error of the two-mode entanglement transformation Controlled-Z by introducing non-Gaussian nodes in the cluster. Non-Gaussian nodes are obtained by using a cubic phase gate. We have shown that this strategy can significantly decrease the transformation error. The considered implementation of the Controlled-Z operation contains a teleportation scheme with the cubic phase gate. We have shown that the correct selection of phases during measurement allows for lower errors than in the initial teleportation protocol with the cubic phase gate and the original teleportation protocol.

Keywords: one-way quantum computation, continuous variables, two-mode operations, cubic phase gate, non-Gaussian transformations, teleportation.

DOI: 10.61011/EOS.2023.11.58048.5729-23

1. Introduction

One of the promising models of universal quantum computation is one-way quantum computation [1–3]. The use of continuous variables as a carrier of quantum information allows to build schemes, with each access to which we obtain a significant measurement result (deterministic schemes), which cannot be achieved when working with discrete variables. In addition, systems in continuous variables have great potential in terms of their scalability [4–9]. Therefore, in our work we will discuss one-way quantum computation exactly in the continuous variable regime [1].

However, working with continuous quantum systems also has a significant drawback. The main resource for computation is squeezed states. If their squeezing were infinitely large, the computation would be performed without any errors. However, in practice, states with a finite squeezing ratio are used, which leads to errors that distort the computation results. The squeezing that is experimentally achievable at the moment turns out to be insufficient for universal quantum computation: the maximum experimentally achievable squeezing is -15 dB [10], while for computation (without using surface codes and the post-selection procedure) it is required -20.5 dB [11]. The requirement to the resource state can be reduced by using computation schemes that are less sensitive to the initial error. The idea of constructing such schemes is to analyze the computation procedure, identify the nodes that make the most noise in the result, and reduce their contribution to the computation error.

In [12] there was the analysis of possible strategies for decreasing the error of arbitrary single-mode transformations. The first strategy was to correctly select the weight

coefficients of the cluster state on which the transformation is performed. The second approach to decreasing errors was to replace the nodes that contributed the most to the error with non-Gaussian states obtained using a cubic phase gate [13]. Application of these strategies allowed to significantly decrease the errors of arbitrary single-mode transformation.

Another necessary element for realizing universal quantum computation is the two-mode entangling operation [14,15]. In contrast to single-mode operations, it is not required to be able to perform an arbitrary two-mode operation; it is enough to perform any entangling operation. As the implemented two-mode transformation, we chose the Controlled-Z (CZ) [16–18] transformation, which is an analogue of the CNOT operation in discrete variables, which has the maximum entangling power [19]. This raises the question, do error decreasing strategies for single-mode operations apply to two-mode operations? And if so, are there any specifics for the case of two-mode operations? These are the questions we will try to answer in this paper.

This paper is organized as follows. In Section 2 we describe the implementation of the CZ transformation on a weighted four-node cluster. In the same section we will describe the implementation of the CZ transformation on a cluster with non-Gaussian nodes. Then in Section 3 we compare the errors in the considered schemes with other possible implementations of the CZ transformation on various cluster states [20]. Separately, in Section 4 we will review a teleportation protocol with the cubic phase gate and the homodyne phase correction, which is an integral part of the investigated implementation of the CZ transformation.

2. CZ transformation implementation schemes

The goal of the work is to implement a two-mode entangling CZ transformation that can act on arbitrary input states. The CZ transformation operator with the weight coefficient g_{jk} , which acts on the oscillators j and k , has the form

$$\hat{C}_{Z,jk} = e^{2ig_{jk}\hat{x}_j\hat{x}_k}. \tag{1}$$

This operation transforms the quadratures of the input oscillators as

$$\begin{pmatrix} \hat{x}_{out,j} \\ \hat{x}_{out,k} \\ \hat{y}_{out,j} \\ \hat{y}_{out,k} \end{pmatrix} = \begin{pmatrix} 1 & 0 & 0 & 0 \\ 0 & 1 & 0 & 0 \\ 0 & g_{jk} & 1 & 0 \\ g_{jk} & 0 & 0 & 1 \end{pmatrix} \begin{pmatrix} \hat{x}_{in,j} \\ \hat{x}_{in,k} \\ \hat{y}_{in,j} \\ \hat{y}_{in,k} \end{pmatrix}. \tag{2}$$

It is worth noting that implementing a CZ transformation for two arbitrary input states is not equivalent in complexity to entangling squeezed oscillators or entangling input states with a cluster using a CZ transformation. In the latter case, it is required to organize the interaction of quantum states with clearly known properties, which is obviously a simpler task from the point of view of its physical implementation. In optical systems, the CZ operation on cluster nodes is often replaced by correctly selected linear optical transformations [21,22]. However, a CZ operation on an arbitrary pair of states can be performed using an already generated cluster state.

Further, we will review schemes for implementing CZ on a four-node cluster and the possibility of reducing the transformation error by introducing non-Gaussian nodes into the resource cluster state.

2.1. CZ transformation on a weighted four-node cluster

To begin with, let us look at how the CZ transformation is implemented on a weighted linear four-node cluster without using non-Gaussian nodes. This will allow us to determine the parameters at which the CZ transformation is implemented in the circuit. In addition, such an analysis will allow to identify cluster nodes whose contribution to the error cannot be influenced by the weight coefficients of the cluster state. We will subsequently replace these nodes with non-Gaussian ones.

Let us start with constructing the cluster state itself (Fig. 1, a). The resource for its preparation are oscillators squeezed by y -quadrature, the quadratures of which are described by the equations

$$\hat{x}_j = e^r \hat{x}_{0,j}, \quad \hat{y}_j = e^{-r} \hat{y}_{0,j}, \tag{3}$$

where $\hat{x}_{0,j}$ and $\hat{y}_{0,j}$ — quadrature of the j oscillator in a vacuum state. The degree of squeezing of the initial states is considered the same and is set by the parameter r , which determines the proportional stretching and squeezing of the quadratures of the vacuum state of the field. Entangling the

cluster nodes is carried out using the CZ transformation. Let us note that in a real experiment, cluster generation can be carried out using beam splitters [21,22]. However, for simplicity of the discussion, we will preserve the logic of constructing the circuit with CZ transformations. Then the input states are entangled with the generated cluster also due to the CZ transformation.

All CZ operations commute with each other, and the CZ transformation that interchanges the second and third resource oscillators commutes with all homodyne measurements. Due to it, it is possible to reduce the transformation on a four-node cluster (Fig. 1, b) to the transformation on a pair of two-node clusters (Fig. 1, c) with their further entanglement. This will greatly simplify the analysis of the scheme.

In this representation, homodyne measurements on the first input state In_1 and the first resource oscillator S_1 with the phases of the local oscillators θ_1 and θ_2 will lead to the state quadratures in the second channel will be determined by the equation

$$\begin{pmatrix} \hat{x}'_2 \\ \hat{y}'_2 \end{pmatrix} = \begin{pmatrix} \frac{\cot \theta_1 \cot \theta_2}{g_1 g_4} - \frac{g_4}{g_1} & \frac{\cot \theta_2}{g_1 g_4} \\ -\frac{g_1 \cot \theta_1}{g_4} & -\frac{g_1}{g_4} \end{pmatrix} \begin{pmatrix} \hat{x}_{in} \\ \hat{y}_{in} \end{pmatrix} + \begin{pmatrix} -\frac{\hat{y}_1}{g_1} \\ \hat{y}_2 \end{pmatrix} + \begin{pmatrix} I_1 \\ \beta g_1 \sin \theta_2 - \frac{I_{in,1} g_1}{\beta g_2 \sin \theta_1} - \frac{I_{in,1} \cot \theta_2}{\beta g_1 g_2 \sin \theta_1} \end{pmatrix}. \tag{4}$$

Here $I_{in,1}$ and I_1 — measured values of photocurrents in the first input and first resource channels, respectively, β — amplitude of local oscillators of homodyne detectors. A detailed derivation of this relationship is presented in [12]. The oscillator quadratures in the third resource channel will be given by a similar equation. After this, the oscillators in the second and third resource channels are entangling using the CZ operation with a weight coefficient g_2 , and then the c -number components of the quadratures are compensated based on the measurement results.

The scheme under consideration will carry out transformation (2) over the quadratures of the input oscillators, provided $g_4 = -g_1$, $g_5 = -g_3$ and $\theta_1 = \theta_2 = \theta_3 = \theta_4 = \pi/2$. The quadratures of the output oscillators will be given by the equation

$$\begin{pmatrix} \hat{x}_{out,1} \\ \hat{x}_{out,2} \\ \hat{y}_{out,1} \\ \hat{y}_{out,2} \end{pmatrix} = \begin{pmatrix} 1 & 0 & 0 & 0 \\ 0 & 1 & 0 & 0 \\ 0 & g_2 & 1 & 0 \\ g_2 & 0 & 0 & 1 \end{pmatrix} \begin{pmatrix} \hat{x}_{in,1} \\ \hat{x}_{in,2} \\ \hat{y}_{in,1} \\ \hat{y}_{in,2} \end{pmatrix} + \begin{pmatrix} -\frac{\hat{y}_1}{g_1} \\ -\frac{\hat{y}_4}{g_3} \\ \hat{y}_2 - g_2 \frac{\hat{y}_4}{g_3} \\ \hat{y}_3 - g_2 \frac{\hat{y}_1}{g_1} \end{pmatrix}. \tag{5}$$

In this equation, the first term on the right side is responsible for the transformation over the input quadratures. We see that the weight coefficient of the implemented CZ transformation will depend only on the weight coefficient of the cluster state g_2 . At the same time, the second term on the right side of equation (5) is the error vector $\delta \hat{\mathbf{e}}_1$, depending on the non-ideally squeezed quadratures of the original resource oscillators from which the cluster state is generated.

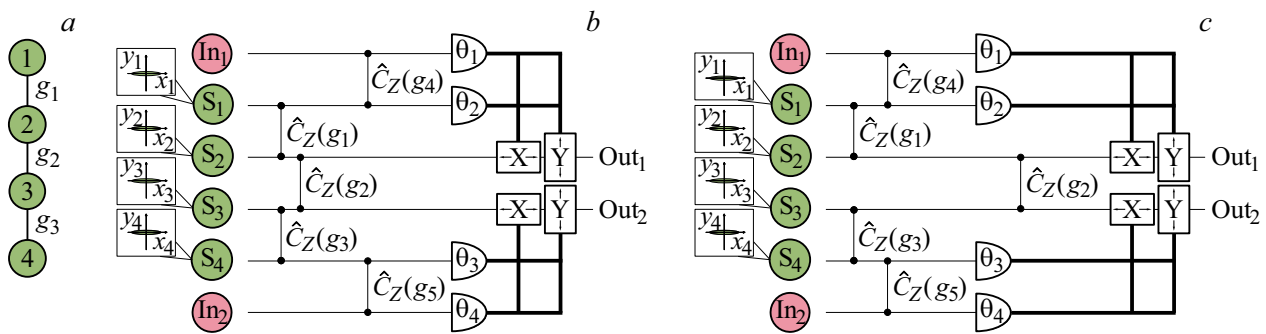


Figure 1. (a) The structure of the cluster state used as a resource. (b) Scheme for implementing the CZ transformation on a linear weighted four-node cluster. (c) Scheme for implementing the CZ transformation on a pair of two-node clusters. In schemes: In_j — input states, S_j — oscillators, squeezed by y -quadrature; $\hat{C}_Z(g_j)$ — CZ transformations with weight coefficients g_j ; θ_j — homodyne measurement with corresponding local oscillator phase; X and Y — displacement operations that displace the corresponding field quadratures depending on the results of the homodyne measurement.

Let us evaluate the errors in the scheme under consideration. To do this, let's move from the error vector $\delta \hat{e}_1$ to a vector consisting of mean square error fluctuations in each of the quadratures $\langle \delta \hat{e}_1^2 \rangle$. We will assume that all Gaussian resource states are squeezed in the same way, that is, $\langle \delta \hat{y}_j^2 \rangle \equiv \langle \delta \hat{y}_s^2 \rangle$ for $j \in 1, 2, 3, 4$. Since we must perform the CZ operation with a fixed weight coefficient, g_2 cannot act as an optimization parameter. Therefore, for simplicity, we will review the case of $g_2 = 1$. Then the vector of mean-square error fluctuations for such a CZ implementation has the form

$$\langle \delta \hat{e}_1^2 \rangle = \begin{pmatrix} \frac{1}{g_1^2} \\ \frac{1}{g_3^2} \\ 1 + \frac{1}{g_3^2} \\ 1 + \frac{1}{g_1^2} \end{pmatrix} \langle \delta \hat{y}_s^2 \rangle. \tag{6}$$

As we can see, the error of the two-mode transformation will decrease as the weight coefficients g_1 and g_3 increase. Ideally, it is possible to achieve zero error in the x -quadratures of the output states, but the error in the y -quadratures cannot be made less than the dispersion of the squeezed quadratures of the resource oscillators $\langle \delta \hat{y}_s^2 \rangle$. The source of this error is the non-ideally squeezed quadratures of the second and third resource oscillators, since we cannot reduce their contribution to the error by choosing the weight coefficients.

It can be noted that the CZ implementation under consideration contains two teleportation schemes that carry input states to the second and third resource oscillators. The transformation error will directly depend on the error with which the teleportation procedure is performed.

It is worth noting that for a two-mode transformation there is no requirement for the relationships between the weight coefficients of the cluster state, as was the case for single-mode operations [12]. This is because each of the weight coefficients is effectively involved in a separate independent process: g_1 and g_3 — in teleportation of input states In_1 and In_2 , respectively, g_2 — in entangling states after teleportation.

2.2. CZ transformation scheme with the cubic phase gate

As we found out in the previous section, increasing the weight coefficients does not make it possible to decrease the error in the y -quadratures of the output states. However, the scheme shown in Fig. 1, c contains two teleportation protocols using the CZ transformation as an entangling operation [23]. It was shown in [24] that it is possible to decrease the error in the teleportation protocol by using non-Gaussian resource states obtained by using a cubic phase gate. We use the same approach to decrease the CZ transformation error. That is, we replace the cluster nodes that make the greatest contribution to the error with non-Gaussian resource states. Since increasing the weight coefficients does not affect the error introduced by the second and third resource oscillators, we will replace them (Fig. 2, a).

The non-Gaussian resource states themselves are prepared by sequentially applying operations as shown in Fig. 2, b. To obtain the required non-Gaussian state from a Gaussian resource oscillator with number j , first it is required to apply a phase rotation operation by $\pi/2$:

$$\hat{R}_{\pi/2,2} = e^{i\frac{\pi}{2}a_2^\dagger a_2}. \tag{7}$$

After this, we apply the displacement operation along the y -quadrature by the value $\alpha > 0$, the operator of which has the form

$$\hat{Y}_{\alpha,j} = e^{2i\alpha\hat{x}_j}. \tag{8}$$

The preparation procedure is completed by the action of the non-Gaussian operation — cubic phase gate, its operator is determined by the equation

$$\hat{Q}_{\gamma,j} = e^{-2i\gamma\hat{y}_j^3}, \tag{9}$$

where γ — real coefficient characterizing the degree of non-linearity of the transformation. After such transformations, the j th resource oscillator will go into a non-Gaussian state. The action of a cubic phase gate deforms the uncertainty

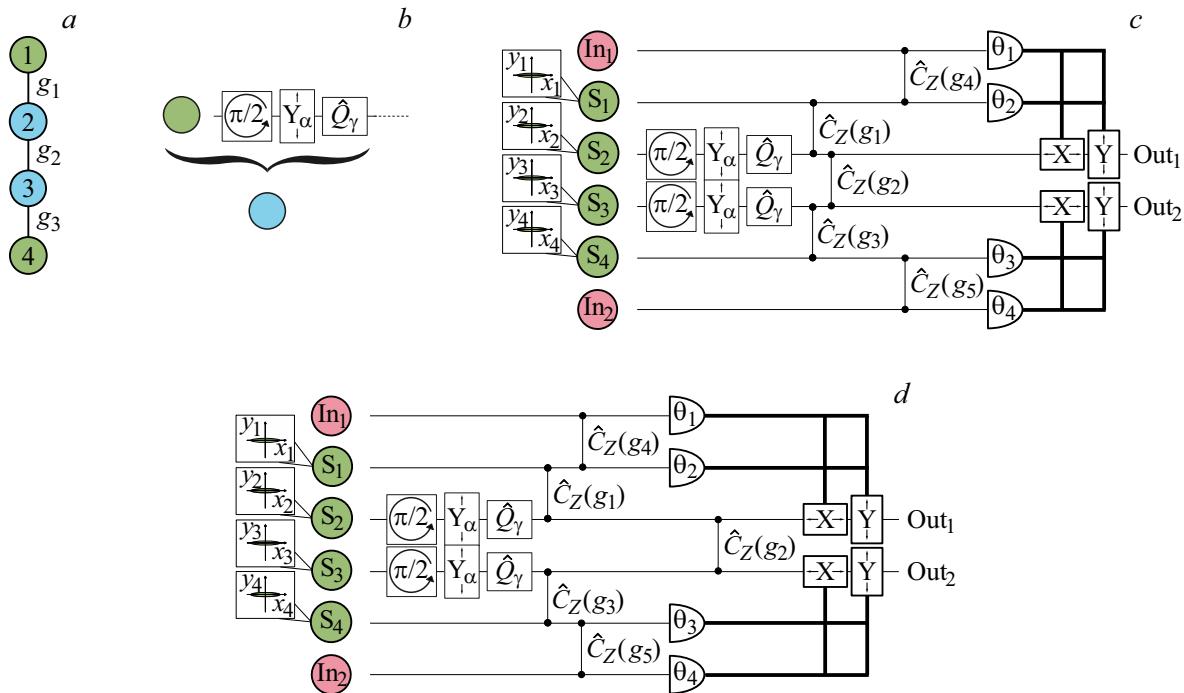


Figure 2. (a) The structure of the cluster state used as a resource for calculation: Gaussian nodes are shown in green, non-Gaussian nodes in blue. (b) Scheme for preparing a non-Gaussian resource state. (c) Scheme of the implementation of the CZ transformation on a linear weighted four-node cluster using a cubic phase gate. (d) Scheme of the implementation of the CZ transformation on a pair of two-node clusters using a cubic phase gate. In schemes: Y_α — displacement operation of y -quadrature by the value α , \hat{Q}_γ — a cubic phase gate with the degree of the nonlinearity γ .

region of the state squeezed along the x -quadrature in such a way that a parabola is formed on the phase plane. However, when displaced along the y -quadrature by a positive value α , satisfying the condition $\alpha^2 \gg \langle \hat{x}_j^2 \rangle$, the quadrature values of the second oscillator will lie in the first quadrant of the phase plane. In other words, only one of the branches of the parabola will remain on the phase plane.

The complete implementation of CZ transformation using a cubic phase gate is shown in Fig. 2, c. Just as in the previous section, we can move on to an equivalent transformation scheme on a pair of two-node clusters (Fig. 2, d). Since the operations performed on input states on two-node clusters are similar to each other, we will only consider how In_1 is transformed. After the action of operators (7)–(9), the second resource oscillator will go into a non-Gaussian state, the amplitude of which is described by the equation

$$\hat{a}_2 = -\hat{y}_2 + 3\gamma(\alpha + \hat{x}_2)^2 + i(\alpha + \hat{x}_2). \quad (10)$$

In order to teleport the state In_1 to the second resource oscillator, it is required that $g_4 = -g_1$ when entangling. After entangling by two CZ operations, the amplitudes of the oscillators are described by the equations

$$\hat{a}'_{in} = \hat{x}_{in} + i(\hat{y}_{in} - g_1\hat{x}_1), \quad (11)$$

$$\hat{a}'_1 = \hat{x}_1 + i(\hat{y}_1 - g_1\hat{y}_2 + 3g_1\gamma(\alpha + \hat{x}_2)^2 - g_1\hat{x}_{in}), \quad (12)$$

$$\hat{a}'_2 = -\hat{y}_2 + 3\gamma(\alpha + \hat{x}_2)^2 + i(\alpha + \hat{x}_2 + g_1\hat{x}_1). \quad (13)$$

We see that the first resource oscillator now contains the nonlinearity from the non-Gaussian oscillator due to entanglement. Then homodyne measurements are carried out with the phases of the local oscillators θ_1 and θ_2 over the input and first resource oscillators, respectively. In this case, we set $\theta_2 = \pi/2$, as was done in the previous section. However, we will not fix the angle θ_1 ; we will need the ability to vary this angle in the future. The photocurrent operators for such measurements will have the form:

$$\hat{i}_{in} = \beta \sin \theta_1 (\hat{y}_{in} - g_1\hat{x}_1) + \beta \cos \theta_1 \hat{x}_{in}, \quad (14)$$

$$\hat{i}_1 = \beta (\hat{y}_1 - g_1\hat{y}_2 + 3g_1\gamma(\alpha + \hat{x}_2)^2 - g_1\hat{x}_{in}). \quad (15)$$

Let the measured values of photocurrents \hat{i}_{in} and \hat{i}_1 be equal to I_{in} and I_1 , respectively. Then the quadratures of the second oscillator after measurements will be determined by the equations:

$$\hat{x}'_2 = \hat{x}_{in} - \frac{\hat{y}_1}{g_1} + \frac{I_1}{\beta g_1}, \quad (16)$$

$$\hat{y}'_2 = \cot \theta_1 \hat{x}_{in} + \hat{y}_{in} - \frac{I_{in}}{\beta \sin \theta_1} + \frac{1}{\sqrt{3\gamma}} \sqrt{\frac{I_1}{\beta g_1} + \hat{x}_{in} - \frac{\hat{y}_1}{g_1} + \hat{y}_2}. \quad (17)$$

Due to the non-Gaussian resource, a root appears in equation (17), which determines the transformation error.

Let us note that due to the large value of the displacement α , only the positive value of the root needs to be taken into account.

We can decompose the root in equation (17) into a series with respect to the parameter,

$$\frac{\beta g_1}{I_1} \left(\hat{x}_{in} - \frac{\hat{y}_1}{g_1} + \hat{y}_2 \right), \tag{18}$$

retaining only the first term in the decomposition, that is

$$\begin{aligned} \hat{y}'_2 = & \cot \theta_1 \hat{x}_{in} + \hat{y}_{in} - \frac{I_{in}}{\beta \sin \theta_1} + \sqrt{\frac{I_1}{3\gamma\beta g_1}} \\ & + \sqrt{\frac{\beta g_1}{12\gamma I_1}} \left(\hat{x}_{in} - \frac{\hat{y}_1}{g_1} + \hat{y}_2 \right). \end{aligned} \tag{19}$$

Termination of the series is correct under the assumption that all moments of the decomposition parameter are small. For Gaussian input states, it is sufficient to satisfy the inequalities

$$3\gamma\alpha^2 \gg \langle \hat{x}_{in} \rangle, \tag{20}$$

$$(3\gamma\alpha^2)^2 \gg \langle \hat{x}_{in}^2 \rangle + \frac{\langle \hat{y}_1^2 \rangle}{g_1^2} + \langle \hat{y}_2^2 \rangle. \tag{21}$$

Let us note that this requirement limits the applicability of the protocol under consideration. However, it can be satisfied for the class of input states of interest to us due to the correct choice of the value α .

As a result, the quadratures of the input state are transformed as follows:

$$\begin{aligned} \begin{pmatrix} \hat{x}'_2 \\ \hat{y}'_2 \end{pmatrix} = & \begin{pmatrix} 1 & 0 \\ \cot \theta_1 + \sqrt{\frac{g_1\beta}{12\gamma I_1}} & 1 \end{pmatrix} \begin{pmatrix} \hat{x}_{in,1} \\ \hat{y}_{in,1} \end{pmatrix} \\ & + \begin{pmatrix} -\frac{\hat{y}_1}{g_1} \\ \sqrt{\frac{g_1\beta}{12\gamma I_1}} \left(\hat{y}_2 - \frac{\hat{y}_1}{g_1} \right) \end{pmatrix} + \begin{pmatrix} \frac{I_1}{\beta g_1} \\ -\frac{I_{in}}{\beta \sin \theta_1} + \sqrt{\frac{I_1}{3\gamma\beta g_1}} \end{pmatrix}. \end{aligned} \tag{22}$$

As you can see, the first term, which describes the transformation itself performed on the input state, contains a matrix element that depends on the measurement results. This results in occasional unwanted transformation distortion. If we do not compensate for this distortion, it will lead to an increase in the error of the transformation being performed. It is possible to compensate for this distortion by choosing the correct measurement basis. Let us note that the value of the photocurrent I_1 is obtained as a result of measurements on the state in the first channel. If we measure the first oscillator before the input one, we can adjust the phase of θ_1 so that

$$\cot \theta_1 = -\sqrt{\frac{g_1\beta}{12\gamma I_1}}. \tag{23}$$

This allows to teleport without uncontrolled distortion.

Thus, by implementing a two-mode CZ transformation, we can correct the uncontrolled distortion caused by the presence of a cubic phase gate in the second resource

channel directly from measurements taken on states in the first input and first resource channels. This situation differs significantly from the case of single-mode operations [12]. An arbitrary single-mode transformation on a four-node cluster can be reduced to two sequential operations on two-node clusters. If we replace one of the nodes of the first cluster with a non-Gaussian state, it will lead to the appearance of distortion as in equation (22). Since we need to be able to implement any single-mode transformation, we should be able to set any phase values for homodyne detectors. Because of this, it is not possible to compensate for the distortion by correcting the phase during measurements in the first transformation on a two-mode cluster and it is required to eliminate it by choosing a basis in subsequent measurements. If we introduced a non-Gaussian resource into the second cluster state, we would not be able to compensate for the distortion caused by it. As a result, it is possible to replace only one node of the original four-node cluster with a non-Gaussian state without consequences. For a two-mode transformation, it is possible to replace both nodes with non-Gaussian states, the contribution to the error from which cannot be suppressed due to the weight coefficients of the cluster state.

The transformation over the second input state In_2 is performed in the same way. After this, the oscillators in the second and third resource channels are entangled using the CZ operation with a weight coefficient g_2 , and then the c -number components of the quadratures are compensated based on the measurement results. As a result, the quadratures at the output of such a CZ transformation scheme will be determined by the equation

$$\begin{aligned} \begin{pmatrix} \hat{x}_{out,1} \\ \hat{x}_{out,2} \\ \hat{y}_{out,1} \\ \hat{y}_{out,2} \end{pmatrix} = & \begin{pmatrix} 1 & 0 & 0 & 0 \\ 0 & 1 & 0 & 0 \\ 0 & g_2 & 1 & 0 \\ g_2 & 0 & 0 & 1 \end{pmatrix} \begin{pmatrix} \hat{x}_{in,1} \\ \hat{x}_{in,2} \\ \hat{y}_{in,1} \\ \hat{y}_{in,2} \end{pmatrix} \\ & + \begin{pmatrix} -\frac{\hat{y}_1}{g_1} \\ -\frac{\hat{y}_4}{g_3} \\ \sqrt{\frac{g_1\beta}{12\gamma I_1}} \left(\hat{y}_2 - \frac{\hat{y}_1}{g_1} \right) - g_2 \frac{\hat{y}_4}{g_3} \\ \sqrt{\frac{g_3\beta}{12\gamma I_4}} \left(\hat{y}_3 - \frac{\hat{y}_4}{g_3} \right) - g_2 \frac{\hat{y}_1}{g_1} \end{pmatrix}. \end{aligned} \tag{24}$$

As we can see, the input quadratures are transformed in the same way as in the scheme without non-Gaussian operations (2), but the errors in the y -quadratures are significantly different.

Let us evaluate the errors that arise in the proposed scheme. The displacement of squeezed states during the preparation of non-Gaussian states will be reviewed identical and equal to α . To evaluate, we take the values of the measured photocurrents equal to their average values, that is $I_1 = \langle \hat{i}_{1,m} \rangle \approx 3\beta\gamma g_1\alpha^2$ and $I_4 = \langle \hat{i}_{4,m} \rangle \approx 3\beta\gamma g_3\alpha^2$.

As in the previous section, we take $g_2 = 1$, and the variances of the squeezed quadratures of resource oscillators are the same and equal to $\langle \delta\hat{y}_s^2 \rangle$. Then the vector of mean

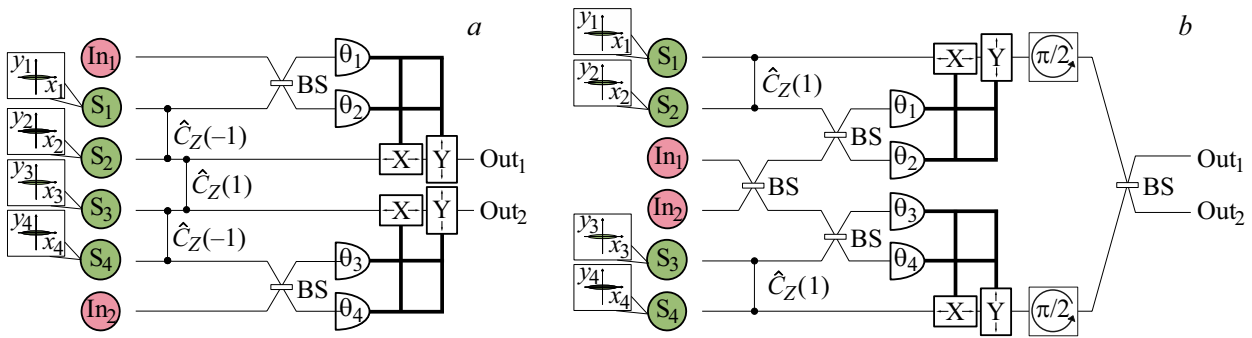


Figure 3. (a) Scheme of the implementation of the CZ transformation on a unweighted four-node linear cluster. (b) Scheme of the implementation of the CZ transformation on a pair of two-node clusters. BS — a symmetrical beamsplitter.

square error fluctuations will have the form

$$\langle \delta \mathbf{e}_2^2 \rangle = \begin{pmatrix} \frac{1}{g_1^2} \\ \frac{1}{g_3^2} \\ \frac{g_1 \beta}{12\gamma I_1} \left(1 + \frac{1}{g_1^2} \right) + \frac{1}{g_3^2} \\ \frac{g_3 \beta}{12\gamma I_4} \left(1 + \frac{1}{g_3^2} \right) + \frac{1}{g_1^2} \end{pmatrix} \langle \delta y_s^2 \rangle$$

$$= \begin{pmatrix} \frac{1}{g_1^2} \\ \frac{1}{g_3^2} \\ \frac{1}{36\gamma^2 \alpha^2} \left(1 + \frac{1}{g_1^2} \right) + \frac{1}{g_3^2} \\ \frac{1}{36\gamma^2 \alpha^2} \left(1 + \frac{1}{g_3^2} \right) + \frac{1}{g_1^2} \end{pmatrix} \langle \delta y_s^2 \rangle. \quad (25)$$

The first term in the y-quadrature errors turns out to be inversely proportional to the measured values of the photocurrents I_1 and I_4 , which increase with increasing displacement α . Thus, we can reduce the contributions to the transformation error from all resource oscillators: from some — due to the weight coefficients of the cluster state, and from others — using a cubic phase gate. Theoretically, this allows to obtain an arbitrarily small transformation error.

3. Comparison of errors of various CZ transformation implementations

Now it is required to compare the errors of different implementations of the CZ transformation on cluster states. We will compare the considered schemes with each other and with the implementations detailed in [20]. The first scheme from [20] (Fig. 3, a) is an implementation of the CZ transformation on an unweighted four-node linear cluster. This implementation is standard for performing two-mode operations on clusters, since the smallest transformation error is achieved when computing on cluster states with the number of nodes twice the number of input nodes [25]. In it, the entangling of input states with the cluster is carried out using beamsplitters. This deprives us of the opportunity to manipulate the weight coefficients of the cluster state and, through them, influence the error. The mean square error

vector for this scheme is determined by the equation:

$$\langle \delta \mathbf{e}_3^2 \rangle = \begin{pmatrix} 2 \\ 2 \\ 3 \\ 3 \end{pmatrix} \langle \delta y_s^2 \rangle. \quad (26)$$

Another scheme implements the CZ transformation on a pair of two-node clusters (Fig. 3, b). This scheme provides the smallest error among those considered by the authors in [20], for it

$$\langle \delta \mathbf{e}_4^2 \rangle = \begin{pmatrix} 2 \\ 2 \\ 2 \\ 2 \end{pmatrix} \langle \delta y_s^2 \rangle. \quad (27)$$

To compare errors for different CZ implementations, we will study the $\| \cdot \|_\infty$ norm as a measure of errors. This norm looks like

$$\| \langle \delta \mathbf{e}_k^2 \rangle \|_\infty = \max_j [\{ \langle \delta \mathbf{e}_k^2 \rangle_j \}]. \quad (28)$$

Now let us discuss the parameter values for error evaluation. In [12] it was shown that with the maximum currently achievable squeezing level -15 dB [10] the values of the weight coefficients of the CZ transformation can lie in the range $[0, 5]$. Since the transformation errors for each of the quadratures in equations (6) and (25) decrease with increasing weight coefficients g_1 and g_3 , then to estimate the norm of errors we will take their maximum possible values $g_1 = g_3 = 5$. To evaluate the error in a scheme with non-Gaussian states, we take the value of the nonlinearity coefficient of the cubic phase $\gamma = 0.1$ [26,27] and the displacement $\alpha = 5\sqrt{5}$ (i.e. $36\gamma^2 \alpha^2 = 45$). This displacement value satisfies the condition $\alpha^2 \gg \langle \hat{x}_j^2 \rangle$ required for the correct operation of the protocol and is feasible in practice [24].

The results of the numerical evaluation are shown in Fig. 4. As you can see, the biggest error will be for implementation on an unweighted cluster. The CZ transformation scheme on a pair of two-node clusters demonstrates an error one and a half times less than the previous case. In the absence of the opportunity of manipulating the cluster weight coefficients, such an implementation provides the

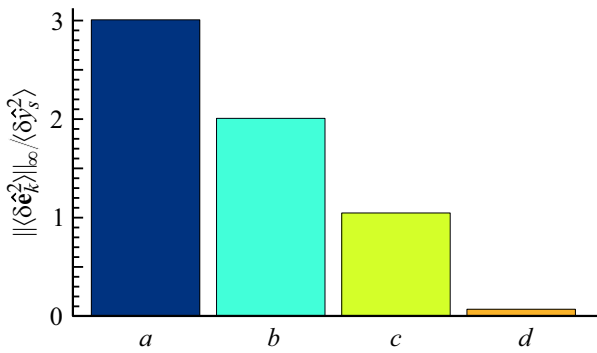


Figure 4. Error in various implementations of the CZ transformation: *a* — on an unweighted four-node linear cluster, *b* — on a pair of two-node clusters, *c* — on a weighted four-node linear cluster, *d* — with a cubic phase gate.

smallest transformation error [20]. At the same time, the implementation of the CZ transformation on a weighted cluster state, which we reviewed in Section 2.1, allows decreasing the error by increasing the weight coefficients of the cluster state. However, even ideally, the error cannot be less than $\langle \delta y_s^2 \rangle$. This scheme provides the smallest error among the implementations we have reviewed that contain only Gaussian transformations. Finally, replacing the nodes in the cluster state that make the largest contribution to the transformation error reduces the amount of noise from all non-ideally squeezed resource oscillators. This strategy allows reducing the error norm by approximately 16 times.

4. Teleportation protocol with the cubic phase gate and the homodyne phase correction

Let us discuss another result that we obtained as a side effect when analyzing the implementation of CZ with non-Gaussian states in Section 2.2. As already mentioned, the CZ transformation scheme discussed in the previous section contains two teleportation schemes. However, the teleportation protocol with cubic phase gate used in this scheme differs from that proposed earlier in [24]. Let us discuss in more detail the modification of the quantum state teleportation protocol that we used in this work and analyze the quality of teleportation.

Let us recall how the original teleportation protocol with the cubic phase gate from [24] works. Its scheme is shown in Fig. 5, *b*. The input state teleportation requires two auxiliary oscillators that are initially squeezed in orthogonal quadratures. First, the state in the second channel is displaced the *y*-quadrature by the value $\alpha > 0$ and the cubic phase gate operation with the degree of nonlinearity γ is applied to it. Next, using CZ transformations, first the resource oscillators are sequentially entangling, and then the input and first resource oscillators; the weight coefficients of the CZ transformations should be g and $-g$, respectively. After it, *y*-quadratures are measured in the input and

first resource channels and, based on the measurement results, the *c*-number components of the quadratures of the unmeasured state are compensated. The state quadratures at the output of this scheme are determined by the equation

$$\hat{x}'_{out} = \hat{x}_{in} - \frac{\hat{y}_1}{g}, \tag{29}$$

$$\hat{y}'_{out} = \hat{y}_{in} + \sqrt{\frac{g}{12\gamma Y_1}} \left(\hat{x}_{in} - \frac{\hat{y}_1}{g} - \hat{x}_2 \right), \tag{30}$$

where Y_1 — the measured value of *y*-quadrature of the first resource oscillator, and \hat{y}_1 and \hat{x}_2 are — squeezed quadratures of the resource oscillators. In these equation, the first terms correspond to the desired teleportation transformation, and the rest determine the transformation error. As we can see, the *y*-quadrature error depends on the *x*-quadrature of the input state, which is generally unknown. As a result, it is this term that makes the greatest contribution to the transformation error.

Now let us consider the teleportation protocol with the cubic phase gate, which is an integral part of the CZ transformation from Section 2.2. Its scheme is show in Fig. 5, *d*. In this modified protocol, we adjust the θ_1 phase value to compensate for uncontrolled distortion of teleportation results. The phase value θ_1 is determined by the equation

$$\cot \theta_1 = -\sqrt{\frac{g}{12\gamma Y_1}}. \tag{31}$$

From equation (22) it follows that the quadratures of the output state in this case have the form

$$\hat{x}_{out} = \hat{x}_{in} - \frac{\hat{y}_1}{g}, \tag{32}$$

$$\hat{y}_{out} = \hat{y}_{in} + \sqrt{\frac{g}{12\gamma Y_1}} \left(\hat{y}_2 - \frac{\hat{y}_1}{g} \right). \tag{33}$$

Comparing these equations with equations (29) and (30), we see that the *x*-quadrature errors are the same, and in the *y*-quadrature error for the protocol with phase correction there is no contribution from the *x*-quadrature of the input state. It is this term that makes the greatest contribution to the transformation error. Moreover, it was the dependence of the error on the input state that was the main limiting factor of the protocol from the work [24]. Here we get rid of this limitation.

To characterize the error level, let us proceed to the values of the mean square fluctuations of the teleportation error in each quadrature, which are defined as $\langle \delta e_x^2 \rangle = \langle (\hat{x}_{out} - \hat{x}_{in})^2 \rangle$ and $\langle \delta e_y^2 \rangle = \langle (\hat{y}_{out} - \hat{y}_{in})^2 \rangle$. As before, we will assume that $\langle \delta y_j^2 \rangle \equiv \langle \delta y_s^2 \rangle$ for $j = 1, 2$, and we will evaluate the value of the measured quadrature as its average, i.e. $Y_1 = \langle \hat{y}_1 \rangle \approx 3\gamma g \alpha^2$. Then the mean square error fluctuations will be given by the equations

$$\langle \delta e_x^2 \rangle = \frac{1}{g^2} \langle \delta y_s^2 \rangle, \tag{34}$$

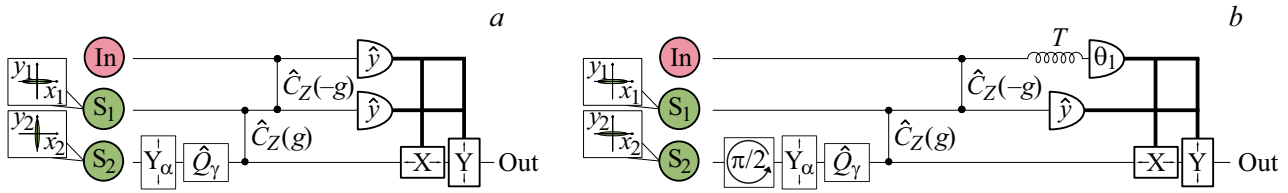


Figure 5. (a) Teleportation scheme using the cubic phase gate. (b) Teleportation scheme with the cubic phase gate and the homodyne phase correction. T — delay line.

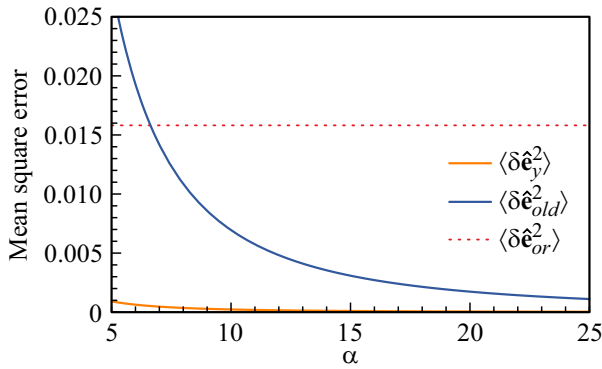


Figure 6. Mean square error y -quadrature of the teleported state depending on the displacement of the non-Gaussian resource α : orange — for the protocol with the phase correction, blue — for the protocol without the phase correction when teleporting the vacuum state. The red dotted line indicates the level of teleportation error in the original scheme. The squeezing level of resource oscillators is -15 dB.

$$\langle \delta \hat{e}_y^2 \rangle = \frac{1 + g^2}{12\gamma g Y_1} \langle \delta \hat{y}_s^2 \rangle = \frac{1 + g^2}{36\gamma^2 \alpha^2 g^2} \langle \delta \hat{y}_s^2 \rangle. \quad (35)$$

The dependence for estimating the mean square fluctuation of the error y -quadrature $\langle \delta \hat{e}_y^2 \rangle$ on the displacement α is shown in orange in Fig. 6. In the calculations, $\gamma = 0.1$, squeezing of resource oscillators -15 dB and $g = 5$ were taken. For comparison, the y -quadrature error $\langle \delta \hat{e}_{old}^2 \rangle$ for the scheme without the homodyne phase correction for the vacuum state teleportation for the same parameters is shown in blue. Red indicates the mean square error fluctuations for the original teleportation scheme $\langle \delta \hat{e}_{or}^2 \rangle = 2 \langle \delta \hat{y}_s^2 \rangle$ [23]. Since at small α the approximations in which the analyzed equations were obtained cease to hold, the dependence in Fig. 6 is plotted for $\alpha > 5$. As we can see, the modified teleportation protocol with the cubic phase gate outperforms its previous version from [24] and the original protocol for any α sufficient to perform the allowed approximations. Thus, correct selection of the phase in homodyne measurements can significantly decrease the error in the teleportation protocol with the cubic phase gate.

5. Conclusion

It is shown that the introduction of non-Gaussian nodes into the cluster state, obtained using a cubic phase gate,

makes it possible to decrease the error when implementing a two-mode entangling CZ transformation on a linear four-node cluster. Moreover, in contrast to the implementation of arbitrary single-mode operations [12] we have the opportunity to reduce the contribution to the error from all resource oscillators. For some oscillators this is achieved by increasing the weight coefficients of the cluster state, and for others by introducing a cubic phase gate into the scheme. Theoretically, this allows to obtain an arbitrarily small transformation error. Numerical estimates for realistic values of the scheme parameters show that the use of a cubic phase gate allows to decrease the transformation error by an order of magnitude relative to a similar implementation containing only Gaussian operations.

Another difference between the implementation of a two-mode CZ transformation and single-mode operations is that it does not require the relationships between the weight coefficients of the cluster state. As a consequence, the task of finding the optimal weight coefficients of the cluster state that ensure the minimum error turns out to be trivial.

The implementation of the CZ transformation under consideration contains a teleportation protocol. This allowed to identify the opportunity of modifying the teleportation protocol with the cubic phase gate, which was proposed earlier [24]. Correct selection of phases during measurement allows to compensate for the distortion caused by the presence of a non-Gaussian operation and which makes the main contribution to the protocol error. As a result, teleportation in the protocol with the cubic phase gate and the homodyne phase correction turns out to be more accurate than in the initial protocol with the cubic phase gate and in the original protocol, and also allows for smaller values of quadrature displacement for error correction.

We cannot but mention the complexity associated with the experimental implementation of the proposed scheme. Its key element is a cubic phase gate, the practical implementation of which is still a challenge for experimenters. The first idea of generating cubic phase states was proposed by Gottesman, Kitaev and Preskill back in 2001 [13,22,28]. However, this method turned out to be difficult to implement experimentally, since it required the operation of displacing quadratures by a value far from what is actually achievable in experiment. Because of this, the cubic phase gate remained for a long time just an abstract mathematical transformation. However, in recent years the situation has changed. More and more works are appearing devoted to new methods for generating states

of the cubic phase [26,29,30] and implementing the cubic phase gate itself [31–35]. Particularly significant successes were achieved in the microwave frequency range — it was in this range that for the first time it was possible to generate a cubic phase state [27]. Thus, the cubic phase gate is gradually evolving from a purely theoretical transformation into a real-life device.

Funding

The study was carried out with financial support from the Foundation for the Development of Theoretical Physics and Mathematics „BASIS“ (grants № 21-1-4-39-1 and № 22-1-5-90-1). S.B. Korolev thanks the Ministry of Science and Higher Education of the Russian Federation and South Ural State University for their support (agreement № 075-15-2022-1116).

Conflict of interest

The authors declare that they have no conflict of interest.

References

- [1] N.C. Menicucci, P. van Loock, M. Gu, C. Weedbrook, T.C. Ralph, M.A. Nielsen. *Phys. Rev. Lett.* **97**, 110501 (2006). DOI: 10.1103/PhysRevLett.97.110501
- [2] R. Raussendorf, H.J. Briegel. *Phys. Rev. Lett.* **86**, 5188 (2001). DOI: 10.1103/PhysRevLett.86.5188
- [3] M.A. Nielsen. *Reports on Mathematical Physics* **57**, 147 (2006). DOI: 10.1016/S0034-4877(06)80014-5
- [4] S. Yokoyama, R. Ukai, S.C. Armstrong, C. Sornphiphatphong, T. Kaji, S. Suzuki, J.-i. Yoshikawa, H. Yonezawa, N.C. Menicucci, A. Furusawa. *Nat. Photon.* **7**, 982 (2013). DOI: 10.1038/nphoton.2013.287
- [5] J. Roslund, R.M. de Araújo, S. Jiang, C. Fabre, N. Treps. *Nat. Photon.* **8**, 109 (2014). DOI: 10.1038/nphoton.2013.340
- [6] M. Chen, N.C. Menicucci, O. Pfister. *Phys. Rev. Lett.* **112**, 120505 (2014). DOI: 10.1103/PhysRevLett.112.120505
- [7] J.-i. Yoshikawa, S. Yokoyama, T. Kaji, C. Sornphiphatphong, Y. Shiozawa, K. Makino, A. Furusawa. *APL Photon.* **1**, 060801 (2016). DOI: 10.1063/1.4962732
- [8] M.V. Larsen, X. Guo, C.R. Breum, J.S. Neergaard-Nielsen, U.L. Andersen. *Science* **366**, 369 (2019). DOI: 10.1126/science.aay4354
- [9] W. Asavanant, Y. Shiozawa, S. Yokoyama, B. Charoensombutamon, H. Emura, R.N. Alexander, S. Takeda, J.-i. Yoshikawa, N.C. Menicucci, H. Yonezawa, A. Furusawa. *Science* **366**, 373 (2019). DOI: 10.1126/science.aay2645
- [10] H. Vahlbruch, M. Mehmet, K. Danzmann, R. Schnabel. *Phys. Rev. Lett.* **117**, 110801 (2016). DOI: 10.1103/PhysRevLett.117.110801
- [11] N.C. Menicucci. *Phys. Rev. Lett.* **112**, 120504 (2014). DOI: 10.1103/PhysRevLett.112.120504
- [12] E.R. Zinatullin, S.B. Korolev, A.D. Manukhova, T.Yu. Golubeva. *Phys. Rev. A* **106**, 032414 (2022). DOI: 10.1103/PhysRevA.106.032414
- [13] D. Gottesman, A. Kitaev, J. Preskill. *Phys. Rev. A* **64**, 012310 (2001). DOI: 10.1103/PhysRevA.64.012310
- [14] S. Lloyd, S.L. Braunstein. *Phys. Rev. Lett.* **82**, 1784 (1999). DOI: 10.1103/PhysRevLett.82.1784
- [15] S.L. Braunstein, P. van Loock. *Rev. Mod. Phys.* **77**, 513 (2005). DOI: 10.1103/RevModPhys.77.513
- [16] M.V. Larsen, J.S. Neergaard-Nielsen, U.L. Andersen. *Phys. Rev. A* **102**, 042608 (2020). DOI: 10.1103/PhysRevA.102.042608
- [17] D. Su, C. Weedbrook, K. Brádler. *Phys. Rev. A* **98**, 042304 (2018). DOI: 10.1103/PhysRevA.98.042304
- [18] R.N. Alexander, S.C. Armstrong, R. Ukai, N.C. Menicucci. *Phys. Rev. A* **90**, 062324 (2014). DOI: 10.1103/PhysRevA.90.062324
- [19] A.T. Reza khani. *Phys. Rev. A* **70**, 052313 (2004). DOI: 10.1103/PhysRevA.70.052313
- [20] S.B. Korolev, T.Yu. Golubeva, Yu.M. Golubev. *Laser Phys. Lett.* **17**, 055205 (2020). DOI: 10.1088/1612-202X/ab83ff
- [21] P. van Loock, C. Weedbrook, M. Gu. *Phys. Rev. A* **76**, 032321 (2007). DOI: 10.1103/PhysRevA.76.032321
- [22] M. Gu, C. Weedbrook, N.C. Menicucci, T.C. Ralph, P. van Loock. *Phys. Rev. A* **79**, 062318 (2009). DOI: 10.1103/PhysRevA.79.062318
- [23] E.R. Zinatullin, S.B. Korolev, T.Yu. Golubeva. *Phys. Rev. A* **103**, 062407 (2021). DOI: 10.1103/PhysRevA.103.062407
- [24] E.R. Zinatullin, S.B. Korolev, T.Yu. Golubeva. *Phys. Rev. A* **104**, 032420 (2021). DOI: 10.1103/PhysRevA.104.032420
- [25] S.B. Korolev, T.Yu. Golubeva, Yu.M. Golubev. *Laser Phys. Lett.* **17**, 035207 (2020). DOI: 10.1088/1612-202X/ab6ffe
- [26] M. Yukawa, K. Miyata, H. Yonezawa, P. Marek, R. Filip, A. Furusawa. *Phys. Rev. A* **88**, 053816 (2013). DOI: 10.1103/PhysRevA.88.053816
- [27] M. Kudra, M. Kervinen, I. Strandberg, S. Ahmed, M. Scigliuzzo, A. Osman, D.P. Lozano, M.O. Tholén, R. Borgani, D.B. Haviland, G. Ferrini, J. Bylander, A.F. Kockum, F. Quijandría, P. Delsing, S. Gasparinetti. *PRX Quantum* **3**, 030301 (2022). DOI: 10.1103/PRXQuantum.3.030301
- [28] S. Ghose, B.C. Sanders. *J. Mod. Opt.* **54**, 855 (2007). DOI: 10.1080/09500340601101575
- [29] Y. Zheng, O. Hahn, P. Stadler, P. Holmval, F. Quijandría, A. Ferraro, G. Ferrini. *PRX Quantum* **2**, 010327 (2021). DOI: 10.1103/PRXQuantum.2.010327
- [30] W. Asavanant, K. Takase, K. Fukui, M. Endo, J.-i. Yoshikawa, A. Furusawa. *Phys. Rev. A* **103**, 043701 (2021). DOI: 10.1103/PhysRevA.103.043701
- [31] K. Marshall, R. Pooser, G. Siopsis, C. Weedbrook. *Phys. Rev. A* **91**, 032321 (2015). DOI: 10.1103/PhysRevA.91.032321
- [32] K. Miyata, H. Ogawa, P. Marek, R. Filip, H. Yonezawa, J.-i. Yoshikawa, A. Furusawa. *Phys. Rev. A* **93**, 022301 (2016). DOI: 10.1103/PhysRevA.93.022301
- [33] R. Yanagimoto, T. Onodera, E. Ng, L.G. Wright, P.L. McMahon, H. Mabuchi. *Phys. Rev. Lett.* **124**, 240503 (2020). DOI: 10.1103/PhysRevLett.124.240503
- [34] T. Hillmann, F. Quijandría, G. Johansson, A. Ferraro, S. Gasparinetti, G. Ferrini. *Phys. Rev. Lett.* **125**, 160501 (2020). DOI: 10.1103/PhysRevLett.125.160501
- [35] S. Konno, A. Sakaguchi, W. Asavanant, H. Ogawa, M. Kobayashi, P. Marek, R. Filip, J.-i. Yoshikawa, A. Furusawa. *Phys. Rev. Applied* **15**, 024024 (2021). DOI: 10.1103/PhysRevApplied.15.024024

Translated by E.Potapova